

The influence of convective outflow on water vapor mixing ratios in the tropical upper troposphere: An analysis based on UARS MLS measurements

J. P. McCormack¹, R. Fu^{1*}, and W. G. Read²

Abstract. The source of increased water vapor mixing ratios over the central and eastern tropical Pacific region during the 1992 El Niño event is examined using measurements of upper tropospheric water vapor provided by the Microwave Limb Sounder (MLS) on board the Upper Atmosphere Research Satellite. Horizontal winds on isentropic surfaces are combined with ISCCP cloud information to provide back-trajectory calculations free of high clouds. These calculations show that the water vapor mixing ratio of an air parcel in the cloud-free regions of the eastern Pacific decreases to approximately one-half of its original value within the first 30 hours after encountering deep convection. This analysis also finds a larger number of air parcels encountering deep convection within 30 hours of observation, and therefore having higher mixing ratios, in March-April 1992 compared to March-April 1994. Hence, increased deep convection over the equatorial central and eastern Pacific in 1992 contributed to the moistening of the downstream tropical upper troposphere.

1. Introduction

The net outgoing longwave radiation is sensitive to changes in humidity that occur in regions of the upper troposphere where the background humidity is low (e.g., [Udelhofen and Hartmann, 1995]). A key question in climate change studies is whether surface warming in the tropics, and a subsequent increase in the frequency and/or intensity of deep convection, would lead to an overall moistening or drying of the tropical upper troposphere [Lindzen, 1990]. Previous studies examining geographic relationships between upper tropospheric humidity, convective cloud amount, and surface temperature either locally or averaged over large spatial scales [Soden and Fu, 1995; Newell *et al.*, 1997; Liao and Rind, 1997; Yang and Tung, 1998] suggest a positive correlation between changes in tropical deep convection and changes in upper tropospheric humidity. Recent theoretical studies [Salathe and Hartmann, 1997; Soden, 1998; Pierrehumbert, 1998; Pierrehumbert and Roca, 1998] have shown that the humidity distribution in these dry regions is primarily determined by vertical and horizontal moisture transport from

regions of convective outflow. These studies dealt with variations in relative humidity over a broad region of the tropical upper troposphere (i.e., 200-500 hPa). Presently, it is unclear whether moisture throughout the uppermost troposphere (above 300 hPa) will change uniformly in response to changes in convection, or whether this response will be dependent on altitude. To address this point, measurements with more accurate vertical registration are needed. The MLS water vapor measurements are capable of focusing on a specific region of the upper troposphere centered near 215 (± 25) hPa.

In the present study, we diagnose the origins of water vapor anomalies and their proximity to regions of deep convection using isentropic back trajectory calculations. The results of these calculations are combined with cloud information and the MLS observations to derive a relationship between an air parcel's water vapor mixing ratio and the time elapsed since it encountered deep convection. This relationship illustrates how changes in the transport of water vapor from a convectively active region moistened the upper troposphere over the central and eastern tropical Pacific during the 1992 warm El Niño/Southern Oscillation (ENSO) event.

2. Data

The UARS MLS instrument utilizes a limb-scanning technique to passively monitor the 205 GHz band, which is sensitive mostly to emissions from the N₂, O₂, and water vapor continua [Read *et al.*, 1995]. For the present study, we utilize MLS water vapor retrievals at three discrete levels: 315 hPa, 215 hPa, and 147 hPa. The retrieval weighting functions at each level are ~ 3 km wide in the vertical direction. Single profile measurement precision is 5 ppmv or less [Newell *et al.*, 1997]. The Version 490 MLS water vapor retrievals presented here are derived from an improved retrieval algorithm; differences between this and earlier versions are described by [Sandor *et al.*, 1998]. Here individual MLS water vapor profiles are first screened to exclude retrievals degraded by the presence of mid- and low-level clouds. Additional quality control rejects retrieved values at 315 hPa when the relative humidity at that level is less than the single layer first-guess value by 5%. A complete description of the Version 490 MLS product is forthcoming [Read *et al.*, manuscript in preparation]. The MLS instrument offers nearly continuous coverage between 34° S and 34° N latitude from September 1991 through October 1995. To compare upper tropospheric water vapor with tropical convective activity, we examine daily global analyses of cloud characteristics provided by the ISCCP D1 data set [Rossow *et al.*, 1996]. Back trajectory calculations are performed to diagnose the dynamical origin of air parcels within the tropical upper troposphere sampled by the MLS. These calculations are based on 6-hourly horizontal wind fields on the 350 K isentropic surface produced by the National Cen-

¹Institute of Atmospheric Physics, University of Arizona, Tucson

²Jet Propulsion Laboratory, California Institute of Technology, Pasadena

*Now at School of Earth and Atmospheric Sciences, Georgian Inst. of Technology.

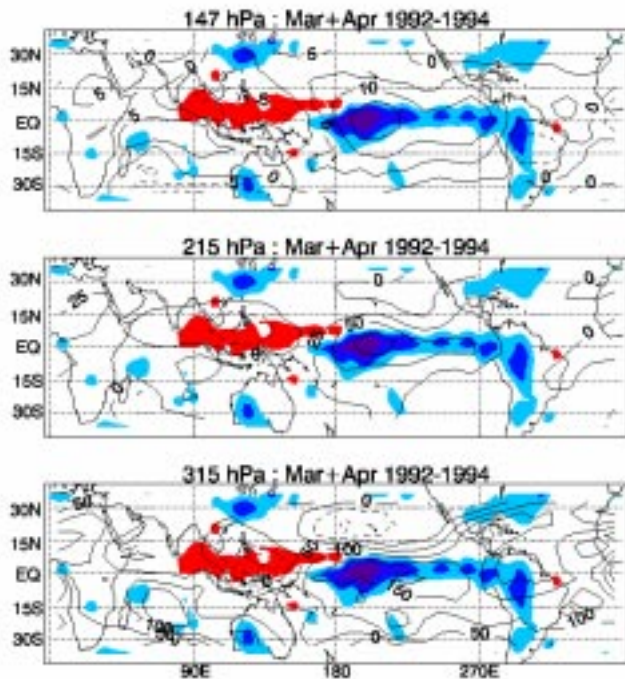


Figure 1. 1992 minus 1994 differences in March-April MLS water vapor mixing ratios at 147 hPa, 215 hPa, and 315 hPa. Contour intervals are drawn every 5, 25, and 50 ppmv, respectively. Solid (dashed) contours represent positive (negative) differences. Blue (red) shading indicates positive (negative) differences in deep convective cloud fraction over the same period.

ters for Environmental Prediction (NCEP) reanalysis project [Kalnay *et al.*, 1996].

3. Observations

[Newell *et al.*, 1997] found differences in MLS 215 hPa water vapor mixing ratios of 20–40 ppmv occurring in the central and eastern tropical Pacific between April 1992 and April 1994. Higher water vapor amounts observed during the 1992 period coincided with the warm ENSO phase in equatorial Pacific sea surface temperatures. The geographical characteristics of this feature at all three pressure levels can be seen in maps of the change in March–April mean MLS water vapor and deep convective cloud fraction between 1992 and 1994 (Figure 1). The region of enhanced convection centered over the equatorial central Pacific and extending eastward to South America corresponds to the regions of maximum water vapor change observed at the three levels. Similarly, regions of suppressed tropical convection extending westward from the dateline to approximately 90° E longitude coincide with areas of decreased MLS water vapor. In the eastern tropical Pacific region, the area of increased water vapor at all three levels extends from approximately 15° S – 25° N and 240° – 270° E. This area is approximately 3000 km to the east of the maximum in convective activity and is broader in latitude than the region of increased convective cloud amount. The back trajectory calculations presented in the following section will focus on this region. That the water vapor differences shown in Figure 1 are representative of ENSO variability can be seen when comparing them with results derived from much longer data sets (e.g., comparing Figure 1c and Figure 8 of Bates *et al.*, [1996]).

4. Back Trajectory Calculations

Isentropic back trajectory calculations are combined with ISCCP cloud information to: (1) describe the relationship between water vapor mixing ratios of air parcels sampled by MLS and the time elapsed since they encountered deep convection; and (2) diagnose any changes in the transport of water vapor away from deep convective regions that may have contributed to the observed differences over the eastern Pacific between the 1992 and 1994 periods (Figure 1).

The MLS retrieval is most reliable at the 215 hPa level, where water vapor mixing ratios generally range between 100–300 ppmv [Read *et al.*, 1995]. At this level, the retrieval uncertainties are clearly smaller than the magnitude of the observed variations from year to year (Figure 1b). In the tropics, the 215 hPa pressure level lies near the 350 K isentropic surface. Assuming that an air parcel in clear regions of the tropics near 215 hPa cools at the rate of $\sim 1 \text{ K day}^{-1}$ [Holton, 1992], the parcel's subsidence rate is on the order of $\sim 10 \text{ hPa day}^{-1}$. After five days, the amount of subsidence could be comparable with the width of the MLS weighting function at 215 hPa, which peaks between 190 hPa and 240 hPa. Therefore, we select an upper limit of five days for the range of the back trajectory calculations. The amount of subsidence over this period should be small enough to allow winds from the 350 K isentropic surface and water vapor information from the 215 hPa level to be representative of conditions encountered by a parcel along its back trajectory.

For each UARS measurement day during March–April 1992 and 1994, the location of an individual MLS profile falling within our region of interest (i.e. 240° – 270° E, 15° S – 25° N) becomes the origin of a back trajectory. Each calculation is carried out for five days at three-hour intervals using interpolated winds. At each interval, the value of the ISCCP D1 deep convective cloud fraction for the corresponding location is recorded. Each trajectory is then examined for values

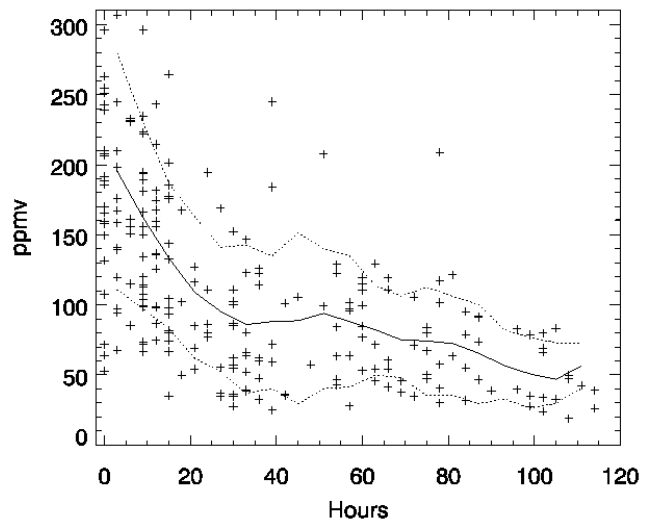


Figure 2. MLS water vapor measurements at the origin of each 350 K back trajectory versus the time elapsed since the parcel encountered deep convection during January–April 1992. Values from trajectories free of high cloud are plotted as individual points along with the means (solid line) and 1-sigma (dotted lines) standard deviations for 6-hour intervals.

of daytime deep convective cloud fraction exceeding 15%. At the first occurrence of this value, the MLS 215 hPa water vapor mixing ratio at the origin is compared with the time elapsed since the parcel last encountered a region of active convection.

5. Results

We first examine more than 700 trajectories originating within the region of interest between January and April 1992. When all trajectories are considered, there is a large scatter in the MLS water vapor mixing ratio as a function of time elapsed since convection was encountered, and thus no clear relationship emerges.

The presence of cirrus clouds along the back trajectories complicates the assumption of isentropic transport, either through the evaporation of ice particles in the dry cloud free regions or through diabatic heating anomalies [Sherwood, 1999]. We account for this by screening each back trajectory for the presence of high clouds (i.e. cloud-top pressures < 310 hPa) using the ISCCP D1 cloud data set. If a parcel far from a region of (daytime) deep convection encounters a region where the high cloud fraction exceeds 5% then that trajectory is disregarded on the grounds that cirrus clouds may be present. When only those back trajectories free of high clouds are considered, a relationship emerges between 215 hPa water vapor mixing ratio sampled by MLS and the elapsed time since this air last encountered deep convection (Figure 2). On average, the mixing ratios of parcels at 215 hPa that encountered deep convection within thirty hours of being sampled by MLS are approximately 50 ppmv higher than the mixing ratios of parcels encountering convection after more than thirty hours. Because of the uncertainties in the MLS retrievals and the assumptions made in the back trajectory calculations, we emphasize the qualitative nature of the result plotted in Figure 2.

Figure 3 shows the locations where air parcels originating within the boxed region encounter daytime deep convection (cloud fraction > 15%) following the 350 K isentropic back trajectories computed during March-April 1992 (Figure 3, top) and 1994 (Figure 3, bottom). A larger number of

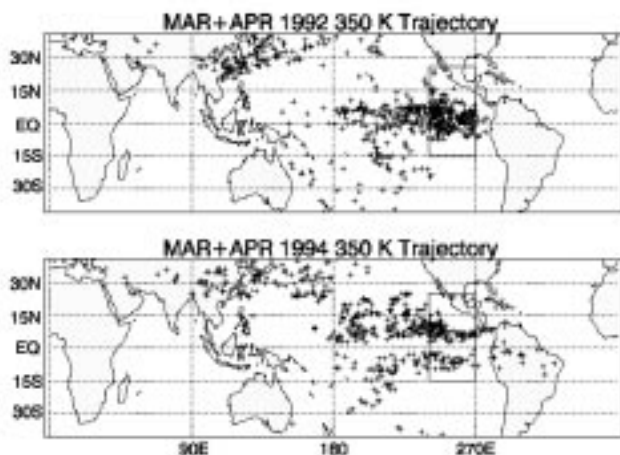


Figure 3. The locations of deep convection along individual 350 K isentropic back trajectories. All trajectories originate within the boxed region and are based on wind and cloud fields for March-April 1992 (top panel) and March-April 1994 (bottom panel).

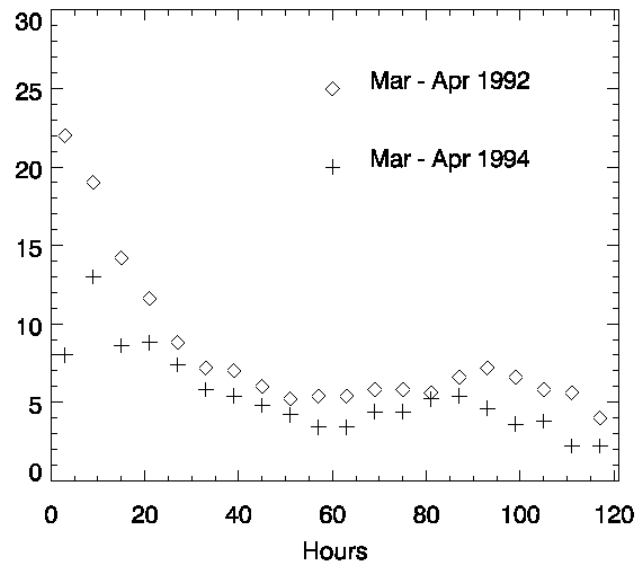


Figure 4. Frequency distribution of the number of trajectories (from Figure 3) encountering deep convection within 6-hour bins from zero to 120 hours for the March-April periods of 1992 and 1994.

parcels encounter active convection over the equatorial eastern Pacific region in 1992 compared to 1994. The eastward shift in the center of deep convection associated with the 1992 warm ENSO event apparently moves the source of upper tropospheric water vapor closer to where enhanced water vapor amounts are observed in March-April 1992. To verify this, we determine the number of back-trajectories originating in this region that have encountered deep convection within six-hour intervals from zero out to 120 hours. As Figure 4 shows, there is a larger number of parcels encountering deep convection within 30 hours during the March-April 1992 period as compared to the March-April 1994 period. The amount of subsidence should be small compared to the width of the MLS weighting function at 215 hPa within this initial thirty hour interval.

6. Conclusion

In the present study we examine MLS water vapor retrievals for the region of the upper troposphere near 215 hPa and assume that the history of an air parcel sampled by MLS can be traced from isentropic flow on the 350 K surface over relatively short time periods (< 5 days). We have found that when the elapsed time since encountering deep convection is in the range of 20-30 hours, a parcel's mixing ratio is reduced by roughly a factor of two compared to air parcels which have just exited from a convective region (Figure 2). For typical atmospheric conditions near 215 hPa in the tropics over the March-April period, it would take approximately 4-5 days for a parcel's mixing ratio to decrease by a factor of two due to subsidence alone, assuming a cooling rate of $\sim 1 \text{ K day}^{-1}$. Because the trajectories have been screened for the presence of high cloud, this observed decrease within the first 20-30 hours is presumably due primarily to mixing with surrounding dry air in the cloud free regions. The mixing ratios of air parcels more than two days removed from a convective region are about one-third to one-quarter of values for air parcels just exiting convection.

During the March-April 1992 period, back trajectory calculations focusing on the eastern tropical Pacific region show a larger number of air parcels sampled by MLS had encountered deep convection within the last 30 hours as compared to the March-April 1994 period (Figure 4). The eastward shift in deep convection associated with the 1992 ENSO event thus moistened the downstream region of the tropical upper troposphere. Future work will examine whether the radiative effects of cirrus outflow from convective regions modulate the observed drying, since air parcels encountering regions of high cloud do not exhibit the same decrease in mixing ratio with time as the cloud-free trajectories in Figure 2.

Acknowledgments. This work was supported under NASA grant NAG5-6687.

References

- Bates, J. J., X. Wu, and D. L. Jackson, Interannual variability of upper-troposphere water vapor band brightness temperature, *J. Clim.*, *9*, 427-438, 1996.
- Holton, J. R., *An Introduction to Dynamic Meteorology*, 3rd. ed., 511 pp., Academic Press, New York, 1992.
- Kalnay, E., et al., The NCEP/NCAR 40 Year Reanalysis project, *Bull. Am. Meteorol. Soc.*, *77*, 437-471, 1996.
- Liao, X., and D. Rind, Local upper tropospheric/lower stratospheric clear-sky water vapor and tropospheric deep convection, *J. Geophys. Res.*, *102*, 19,543-19,557, 1997.
- Lindzen, R. S., Some coolness concerning global warming, *Bull. Am. Meteorol. Soc.*, *71*, 1,465-1,467, 1990.
- Newell, R. E., Y. Zhu, W. G. Read, and J. W. Waters, Relationship between tropical upper tropospheric moisture and eastern tropical Pacific sea surface temperature at seasonal and interannual time scales, *Geophys. Res. Lett.*, *24*, 25-28, 1997.
- Pierrehumbert, R. T., Lateral mixing as a source of subtropical water vapor, *Geophys. Res. Lett.*, *25*, 151-154, 1998.
- Pierrehumbert, R. T., and R. Roca, Evidence for control of Atlantic subtropical humidity by large scale advection, *Geophys. Res. Lett.*, *25*, 4,537-4,540, 1998.
- Read, W. G., et al., Upper-tropospheric water vapor from UARS MLS, *Bull. Am. Meteorol. Soc.*, *76*, 2,381-2,389, 1995.
- Rossov, W. B., A. W. Walker, D. E. Beuschel, and M. D. Roiter, International Satellite Cloud Climatology Project (ISCCP) Documentation of New Cloud Datasets, WMO/TD-No. 737, World Meteorological Organization, 115 pp., 1996.
- Salathe, E. P., and D. L. Hartmann, A trajectory analysis of tropical upper-tropospheric moisture and convection, *J. Clim.*, *10*, 2,533-2,547, 1997.
- Sandor, B. J., W. G. Read, J. W. Waters, and K. H. Rosenlof, Seasonal behavior of tropical to midlatitude upper tropospheric water vapor from UARS MLS, *J. Geophys. Res.*, *103*, 25,935- 25,947, 1998.
- Sherwood, S. C., On moistening of the tropical troposphere by cirrus clouds, *J. Geophys. Res.*, *104*, 11,949-11960, 1999.
- Soden, B. J., and R. Fu, A satellite analysis of deep convection, upper-tropospheric humidity, and the greenhouse effect, *J. Clim.*, *8*, 2,333-2,351, 1995.
- Soden, B. J., Tracking upper tropospheric water vapor radiances: A satellite perspective, *J. Geophys. Res.*, *103*, 17,069-17,081, 1998.
- Udelhofen, P. M., and D. L. Hartmann, Influence of tropical cloud systems on the relative humidity in the upper troposphere, *J. Geophys. Res.*, *100*, 7,423-7,440.
- Yang, H., and K. K. Tung, Water vapor, surface temperature, and the greenhouse effect: statistical analysis of tropical-mean data, *J. Clim.*, *11*, 2,686-2,697, 1998.

J. P. McCormack and R. Fu, Institute of Atmospheric Physics, University of Arizona, PO Box 210081, Tucson, AZ 85721-0081. (email: mcc@atmo.arizona.edu)

W. G. Read, Jet Propulsion Laboratory, Mail Stop 183-701, 4800 Oak Grove Drive, Pasadena, CA 91109.

(Received March 23, 1999; revised June 7, 1999; accepted August 10, 1999.)